Modeling and Feedback Control for a Guyed, Flexible, Tubular Lunar Tower

by
Victor Paul Portmann

Submitted to the Department of Mechanical Engineering
in partial fulfillment of the requirements for the degree of
Bachelor of Science
at the
MASSACHUSETTS INSTITUTE OF TECHNOLOGY
June 2023

Authored by: Victor Paul Portmann
Department of Mechanical Engineering
May 19, 2023

Certified by: Dr. Harrison H. Chin
MIT Mechanical Engineering Lecturer, Thesis Supervisor

Accepted by: Professor Kenneth Kamrin
Professor of Mechanical Engineering, Undergraduate Officer

Modeling and Feedback Control for a Guyed, Flexible, Tubular Lunar Tower

by
Victor Paul Portmann

Submitted to the MIT Department of Mechanical Engineering on May 19, 2023
in partial fulfillment of the requirements for the degree of Bachelor of Science

Abstract

The Self-Erecting Lunar Tower for Instruments (SELTI) is a compact, self-deploying composite lunar tower being developed in support of the NASA Artemis campaign. SELTI can elevate instrument payloads for the purposes of navigation, power beaming, communication, sensing, and imaging around permanently shadowed lunar regions. SELTI deploys by unspooling a collapsible carbon fiber composite mast, which transitions into an erect tubular state. Due to variations in the manufacturing process, an 11 m deployment without stabilization exhibits eccentricity and large tip deflections, causing the payload orientation to deviate from a center, upright position. To control the payload orientation, SELTI has guy wires that manipulate the tip position of the tower. It is necessary to develop feedback control for this system to achieve the desired orientation of payload instruments. To facilitate control system development and to mitigate the risk of damaging the tower, a tenth-scale physical model of SELTI was designed and built for experimentation and analytical model verification. The system dynamics were approximated using a “first principles” second order model. The model’s step response was compared to reality to assess the model’s accuracy. A full state feedback controller was created using the analytical model and simulated to demonstrate the improved step response.

Thesis supervisor: Dr. Harrison H. Chin
Title: MIT Mechanical Engineering Lecturer

Acknowledgements

The author would like to express his gratitude to his thesis advisor Dr. Harrison Chin for his continuous support throughout the course of this project. Dr. Chin's expertise in feedback control systems was essential to the progression of the project, and his enthusiasm was invaluable for overcoming the many unforeseen obstacles and tight time constraints.

The author would also like to thank John Zhang, Alex Miller, and George Lordos for their advice and enthusiastic support throughout the entire process of this project and several other projects related to SELTI. Without their devotion to the lunar tower project, the opportunity to pursue this thesis topic would not even exist. These members of the team have always been around to offer up their expertise and moral support. The author would also like to thank Avril Studstill for her integral role in designing the electrical systems for SELTI and the physical model.

The author would also like to express his gratitude to the PI of the Space Resources Workshop that encompasses SELTI, Professor Jefferey Hoffman, and SELTI's point of contact at NASA Langley Research Center, Dr. Juan "Johnny" Fernandez. Dr. Fernandez mentored the author throughout the course of an internship for SELTI development.

This research project was sponsored by the 2020 BIG Idea Challenge, a collaboration between the Space Technology Mission Directorate (STMD), the Game Changing Development Program (GCD), and the Office of STEM Engagement Space Grant Consortium. The author was supported by the Massachusetts Space Grant Fellowship.

Table of Contents

List of Figures

1. Introduction and Background

1.1 Motivation for the Development of Lunar Towers

NASA's Artemis program intends to establish long-term human presence and infrastructure on the moon [3]. To reduce risk of manned missions on the moon, rigorous autonomous exploration must occur beforehand. Permanently shadowed regions (PSRs) near the lunar poles are of interest because of their potential to contain water and nitrogen-rich deposits that could support missions and long-term human presence on the moon [1]. The extreme cold, darkness, and challenging terrain of PSRs poses challenges to missions into these regions. Line of sight between equipment inside and outside of the PSR is likely to be broken by the terrain, complicating the logistics of PSR exploration and resource acquisition. However, the top of a tall tower located just outside a PSR could have line of sight to the sun, Earth, and the lunar surface, inside and outside the PSR [1]. This could enable the use of navigation, power beaming, and communication equipment for missions into PSRs and other challenging regions. Such a tower would have other uses as well, given that it could improve the functionality of any instrument benefiting from a high vantage point or increased line of sight.

1.2 Development of a Lightweight, Stable, Self-Deploying Lunar Tower

The chosen approach to designing a compact, lightweight module that self-deploys into a tall tower was utilizing a thin, unistable carbon fiber composite tube as the deployable tower element. The current system, named the Self-Erecting Lunar Tower for Instruments (SELTI), uses a tube on loan from NASA Langley Research Center (LaRC) that has thin-ply carbon fiber/epoxy plain-weave and unidirectional ply technology, which reduces wall thickness and enables small bending radii, enabling compact stowage [1]. Before deployment, the tube is rolled around a motorized spool in an unstable flattened state. As the spool spins, the carbon fiber is unrolled, pushed upward, and transitioned into its stable state as an erect tube.

Prior to tower deployment, a leveling system consisting of three linear actuator legs in SELTI's base align the direction of tower deployment with the gravity field so that the tube's center of mass is close to the central axis of the deployer to increase stability. SELTI is also equipped with a guy wire system that can be used to stabilize or manipulate the flexible tube. A set of three folding arms, one per guy wire, begin in a stowed state and are extended into a horizontal position prior to tower deployment. Each of the three guy wires is adjusted using a servo motor winch at the base of the corresponding arm. The wires run from the winches, through pulleys in the arms, out the

tips of the arms, and to the top of the carbon fiber tower. A load cell is incorporated in each arm's pulley system to measure the tension of the wire. The arms increase the angle between the tower and the wires, which increases the horizontal tension component desired for providing corrective force and decreases the vertical tension component, which is detrimental because it increases risk of buckling or fracturing the tower.

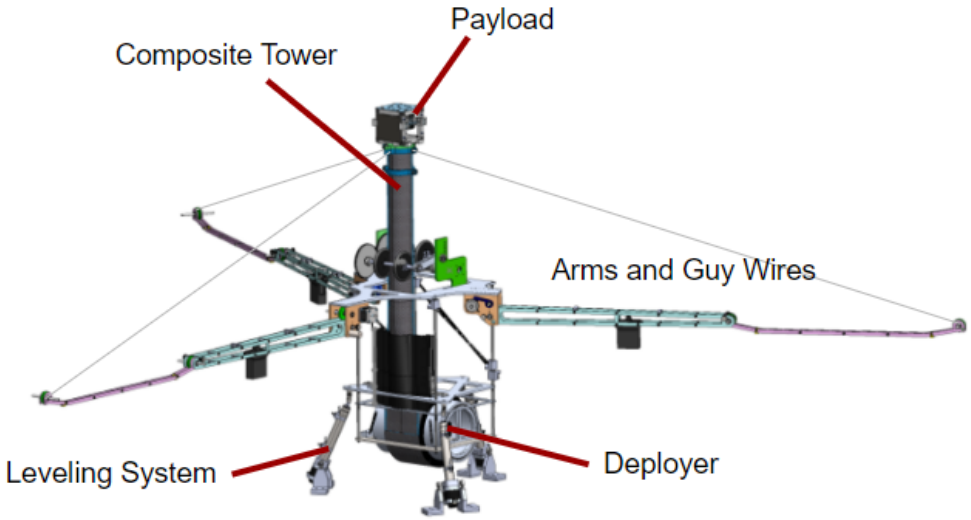

Figure 1-1. Rendering of SELTI from Miller [1]. The major systems and components are labeled. In the state depicted, the folding arms are fully deployed, and the composite tower is stowed.

1.3 Motivation for Developing Feedback Control for the Guyed Tower

Many instruments' effectiveness can be improved by placing them at a high vantage point, but in many cases, orientation is also an important factor for functionality. In the simple example of a video camera in the payload, a high vantage point would provide better visibility, but if pointed in the wrong direction, it is not effective. Therefore, it is necessary to develop a system that is capable of reliably setting payload orientation.

Guyed masts are very common in modern infrastructure on Earth and are used for things like radio towers. These systems typically rely on passive mechanisms to dampen disturbances from the environment, and they can receive maintenance or modifications if necessary. However, manual maintenance is not practical on the moon. Another difference between these scenarios is that, while Earth's guyed towers are typically designed to reject disturbances, disturbances are minimal on the moon due to the lack of an atmosphere. Instead, SELTI's primary purpose is to set the payload instruments in an advantageous position. For these reasons, SELTI would benefit from active payload position control. Whenever the payload orientation is unsatisfactory,

SELTI should be able to automatically readjust and lock the system in its corrected state.

1.4 Guyed System Statics and Dynamics

Irvine [2] presents a scenario in which a cluster of three equally pretensioned guy cables are uniformly spaced around an arbitrary mast (Figure 1-2). Due to wind or other forces on the mast, the junction at which the cables connect to the mast is displaced such that one cable– the “windward guy”– is stretched within the plane it shares with the mast. As a result, tension decreases in the two “leeward guys,” and the guy cables provide a restorative net force on the mast towards the original position with equal cable tensions. This restorative force can be expressed in terms of the guys’ geometry, pretension, and material properties. Equations 1 and 2 are the simplified equations for the horizontal and vertical components, respectively, derived under the assumption that deflections are small [2]. *T* is the pretension of each guy wire; *E* is the Young's modulus of the wires; *A* is the cross sectional area of each cable; and *a*, *b*, *c*, *u*, and *w* are dimensions given in Figure 1-2.

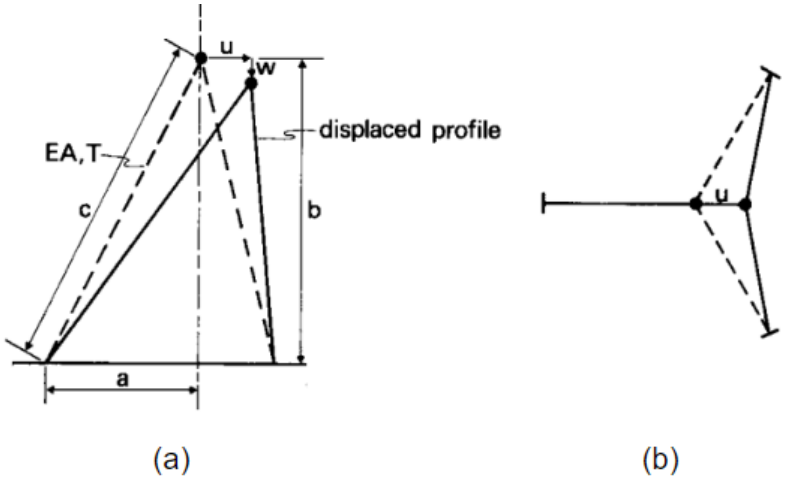

Figure 1-2. Diagrams from Irvine [2]. (a) Side view of the guyed system, showing defined geometries in the plane of windward guy displacement. (b) Top view of the guyed system, showing the horizontal displacements of each guy wire.

$$F_u = [3T + \frac{3}{2}\left(\frac{a}{c}\right)^2 EA]\left(\frac{u}{c}\right) \quad (1)$$

$$F_w = 3T\left(\frac{b}{c}\right) \quad (2)$$

As demonstrated by Huston et al. [4] in a similar study, Irvine's equation for the net lateral force of the guy wire cluster F_u– Equation 1 in the case of three guy wires– can be used to define a spring constant k_c that describes the effective lateral stiffness of the guy wire cluster. Equation 3 provides the effective lateral spring constant for the case of a three-guy-wire cluster with the same properties defined for Equations 1 and 2.

$$k_c = \frac{F_u}{u} = \frac{3}{c}\left[T + \frac{1}{2}\left(\frac{a}{c}\right)^2 EA\right] \tag{3}$$

The effective stiffness k_c of the cable system can be used to derive the equations of motion for the system's lateral displacement [4]. Because SELTI has three equally-spaced guy wires, the previously defined equations are directly applicable to SELTI. The relations provided by Irvine [2] assume that the wires are equally pretensioned, and any changes in tension come only from displacement of the cable junction. This is not necessarily true for SELTI because cable tension can be adjusted using the winches located at the base of each arm. Nevertheless, Irvine's model is useful for estimating guy wire dynamics, especially when the system operates around the initial pretensioned state.

For the analysis of SELTI's dynamics, each guy wire tension is labeled as shown in Figure 1-3, a top view of SELTI analogous to Figure 1-2(b) from Irvine's analysis. The tower's orientation can be manipulated by adjusting these tensions.

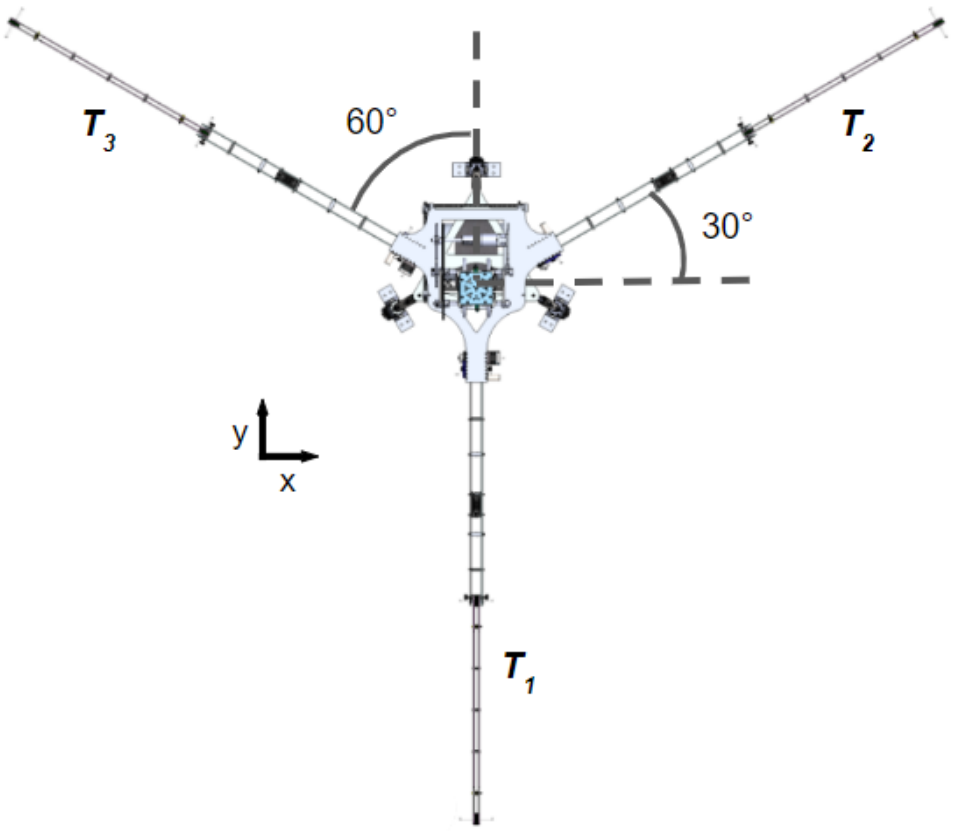

Figure 1-3. Top view of SELTI [1] showing the direction of each guy wire arm and the corresponding tensions used in Equations 4 and 5. In the case of a displacement in the positive y-direction, the "windward guy" defined by Irvine [2] would correspond to the arm with tension T_1.

Following a procedure similar to the methods outlined by Huston et al. [4], the dynamics of the guyed system can be estimated by simple second-order spring-mass-damper models. The inertial parameter is the effective mass of the system m_{eff}, and a damping coefficient B is also defined. SELTI's composite tube has a lenticular cross section, so two different mast stiffnesses k_1 and k_2 are defined for lateral displacements in the x- and y-directions, respectively. The sum of cable cluster stiffness k_c and mast stiffness k_1 or k_2 for a given direction is the total stiffness for that direction, represented as springs in Figure 1-4. The forces acting on the effective mass are the components of guy wire tension acting in the direction of the corresponding model.

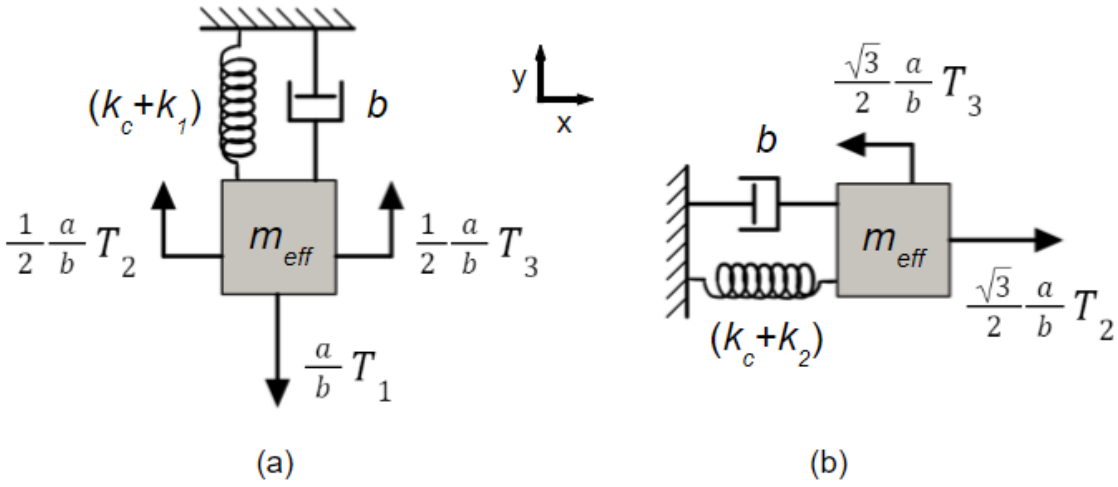

Figure 1-4. Second order spring-mass-damper models describing the dynamics of a deflecting guyed mast with three uniformly spaced, pretensioned guy wires. The one-dimensional models correspond to the components of lateral deflection in the (a) y-direction and (b) x- direction. All wire tension forces are scaled by a factor *a/b* to extract the horizontal component. An additional factor– found using the arm angles labeled in Figure 1-3– is necessary to extract the tension components in the principal directions.

The equations of motion for the second order models in Figure 1-4 are given below in Equations 4 and 5.

$$m_{eff}\frac{d^2u_y}{dt^2} + B\frac{du_y}{dt} + (k_c + k_1)\,u_y = \frac{1}{2}\frac{a}{b}(T_2 + T_3) - \frac{a}{b}T_1 \qquad (4)$$

$$m_{eff}\frac{d^2u_x}{dt^2} + B\frac{du_x}{dt} + (k_c + k_2)\,u_x = \frac{\sqrt{3}}{2}\frac{a}{b}(T_2 - T_3) \qquad (5)$$

Equations 4 and 5 describe the lateral displacements of the cable junction, which– in the case of SELTI– is the top of the tower. However, tilt angle is more crucial for the performance of payload instruments than small-scale positioning. Therefore, the lateral displacements must be converted to equivalent tip angle displacements. The tip deflection *v* and tip angle ϕ of a linear elastic beam– length *L* and stiffness *EI*– under a static load *F* at the tip are given by Equations 6 and 7 below.

$$v = \frac{FL^3}{3EI} \qquad (6)$$

$$\phi = \frac{FL^2}{2EI} \tag{7}$$

Solving for the tip deflection *v* in terms of tip angle ϕ and beam length *L* results in the following equation.

$$v = \frac{2L\phi}{3} \tag{8}$$

Applying this relation to Equations 4 and 5 results in the new equations of motion below. Note that the subscripts are swapped after applying the relation because bending about the x-axis corresponds to lateral displacement in the y-direction and vice versa. There is a sign change in Equation 9 because a displacement in the positive y-direction corresponds to a negative (clockwise) rotation about the x-axis.

$$-\frac{2L}{3}\left[m_{eff}\frac{d^2\phi_x}{dt^2} + B\frac{d\phi_x}{dt} + (k_c + k_1)\,\phi_x\right] = \frac{1}{2}\frac{a}{b}(T_2 + T_3) - \frac{a}{b}T_1 \tag{9}$$

$$\frac{2L}{3}\left[m_{eff}\frac{d^2\phi_y}{dt^2} + B\frac{d\phi_y}{dt} + (k_c + k_2)\,\phi_y\right] = \frac{\sqrt{3}}{2}\frac{a}{b}(T_2 - T_3) \tag{10}$$

Equations 9 and 10 can be used to produce a state space model for estimating the system's response and designing a controller.

2. Experiment Description and Results

2.1 Scaled Physical Model Design

Full deployments of SELTI require significant setup time, as the entire system and required instrumentation must be transported to a suitable location, and many precautionary measures are implemented. Therefore, it is advantageous to have a small model for control system development. Furthermore, SELTI's composite tube endures high stresses during full deployment in Earth's gravity, as exemplified by a fracture that occurred during a deployment experiment [1]. To protect the composite tower and to facilitate control system development, it was decided that testing should be carried out on a low-cost model of SELTI.

For the sake of simplicity, the model should only have to replicate the functionality of the guy wire system and the tower mast. Therefore, the deployer, payload instrumentation, and leveling system were not replicated in the scaled model. Rather, the model was equipped with three sets of guy wires whose tensions are adjusted by winches and measured with load cells.

A model at a scale of 1:10 was chosen to make use of readily available components. An acrylic structure was designed to replicate SELTI's base and arms, and a polyvinyl chloride (PVC) pipe mounted vertically in the acrylic structure takes the place of the composite tower. Due to the composite mast's lenticular cross section, it is stiffer in one axis, and the lower stiffness was used for scaling the model because the tower's deflections are greater in the corresponding direction. To make the model as analogous to SELTI as possible, the bending stiffness EI of the pipe was chosen such that it is a hundredth of SELTI's bending stiffness. The 1:100 scale factor for the model's stiffness was determined using the equations for tip displacement and angle for cantilever beams (Equations 6 and 7). Due to beam length's cubic relationship with tip displacement and square relationship with tip angle, the 1:10 scaling of length and 1:100 scaling of bending stiffness means that, for a given transverse load, the model's tip angle is the same as that of SELTI, and the tip displacement is scaled by 1:10. Thus, in theory, the real tower's displacement profile is consistent with the model, and the orientation of the payload is the same for both. Figure 2-1 is a photo of the physical model.

The physical model also has a mock payload located on top of the pipe with an inertial measurement unit (IMU) for gathering orientation data. It has a cavity for adjusting mass, as well as connection points for the guy wires. A tension spring is included on the end of each guy wire at the connection point so that the effective stiffness of each guy is

lower– approximately equal to the spring stiffness because the Young's modulus of the Spectra® fiber guy wires is very large in comparison, approximately 117 GPa [5].

The stepper motors, load cells, and IMU are controlled by Tinkerforge microcontrollers, which interact with the MATLAB API. The stepper motors are powered by a DC power supply.

Figure 2-1. A photo of the scaled physical model. The stepper motor winches and load cells are located in the acrylic base, and the mock payload is screwed onto the tip of the PVC pipe. The IMU is mounted to the top of the mock payload, and its cable is wired through the pipe. The steppers are powered by a DC power supply.

2.2 Nominal System Parameters

Many of the model parameters (Equations 9 and 10) are known and were directly applied to the model, which was later completed with experimental data. The partially complete model was also used to assess the validity of the analytical approach.

The PVC pipe geometry was chosen such that its bending stiffness EI is approximately 10.5 Nm^2. Its length is 1.5 m. The lateral beam stiffness $k=k_1=k_2$ is equal for displacements in the x- and y-directions due to the pipe's radial symmetry. The beam stiffness k was found by rearranging Equation 6.

$$k = \frac{F}{v} = \frac{3EI}{L^3} \tag{11}$$

Using the nominal parameters, the pipe's lateral stiffness k was found to be approximately 9.33 Nm^{-1}.

The effective mass of the system m_{eff} can be found by adding the payload mass and the inertial contribution from the pipe. As demonstrated by Gurgoze, the effective mass of a vibrating cantilever with uniform linear density is 33/140 of its total mass [6]. The mock payload mass was tuned to 1 kilogram. The combined mass of the PVC pipe and the IMU cable that runs inside of the pipe is approximately 0.76 kg. This results in an effective mass m_{eff} of approximately 1.18 kg.

The stiffness of the guy wire junction is given by Equation 3. Approximating the stiffness of a single guy as the stiffness of the real springs joining the guy cables to the tower k_s=300 Nm^{-1}, the value of k_c is found to be 2.03 Nm^{-1}. The natural frequency ω_n of the second order model is given by the equation

$$\omega_n = \sqrt{\frac{(k+k_c)}{m_{eff}}} \tag{12}$$

The nominal value of ω_n is 3.11 rad/s.

The other known parameters are the geometries defined in Figure 1: arm length a=17 cm, tower height b=L=150 cm, and free cable length c=149 cm.

2.3 System Identification

The physical model was used to collect step response data. To fit parameters to the analytical model, it is necessary to pretension all three guy wires so that the guyed system dynamics can be accounted for by the stiffness k_c. For simplicity, the wires were pretensioned to 1 Newton. Because the PVC pipe has the same bending stiffness in y- and x-directions (pitch and roll, respectively), the parameters used in both second order

models (Equations 9 and 10) are the same. Therefore, all of the parameters can be found using the response to a step input from a single guy wire. Guy wire 1 (labeled in Figure 1-3) was chosen for the step input because, in theory, it only generates a response in pitch. The system's response to a step input– a 90° rotation of the winch, tightening the wire– is shown below in Figure 2-2. The initial pitch is nonzero due to the pipe's eccentricity, and there is an unexpected low frequency component in the response. The low frequency component could be the result of a twisting mode in the pipe and should be further investigated. However, it does not affect the primary mode of the dynamics.

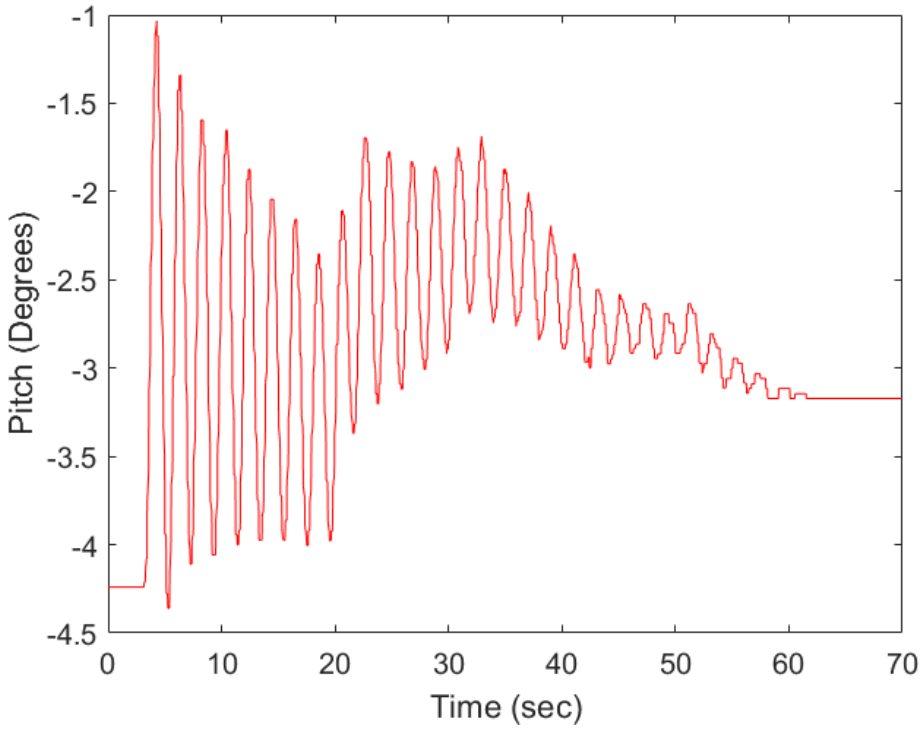

Figure 2-2. Raw data of the step response to a 90° winch rotation in guy wire 1.

Fast Fourier transform was used to find the dominant frequencies, which were found to be 0.0115 Hz and 0.494 Hz. To fit the data to the second order model, a high-pass filter with a passband frequency of 0.494 Hz was applied. This is the damped natural frequency of the second order model ω_d=3.104 rad/s. Along with the nominal natural frequency ω_n (Equation 12), ω_d was used to find the damping ratio using the following relation.

$$\zeta = \sqrt{1 - \left(\frac{\omega_d}{\omega_n}\right)^2} \tag{13}$$

The damping ratio ζ was found to be 0.017. The damping coefficient *B* is given by the equation

$$B = 2\zeta\omega_n m_{eff} \quad (14)$$

and was found to be 0.125 Nsm^{-1}.

The only other unknown parameter was the DC gain K_{dc}, which was found by adjusting the gain to fit the data. The model now had a second order transfer function of the form

$$\frac{\phi_x}{\theta} = \frac{K_{dc}\omega_n^2}{s^2 + 2\zeta\omega_n s + \omega_n^2} = K_{dc}(k + k_c)\frac{1}{m_{eff}s^2 + Bs + (k+k_c)} \quad (15)$$

This transfer function relates pitch ϕ_x to winch rotation θ (both in degrees), but the model represented by Equations 9 relates ϕ_x to wire tension. To establish a connection between the empirical transfer function and the analytical transfer function, the intermediary relationship between winch rotation and wire tension must be accounted for in the model. It can be approximated with Hooke's law, assuming that the tension in the wire is proportional to the wire displacement induced by the winch.

$$\frac{T}{\theta} = r_w k_s \frac{2\pi}{360°} \quad (16)$$

where k_s is the spring constant of the physical springs connecting the guy wires to the model tower, and r_w is the radius of the winch spool. The conversion factor is necessary because θ is in degrees. To match the empirical transfer function with the analytical model, the below relation (Equation 17) must be true. On the right-hand side of the equation, the factor from Equation 9 is scaled by the relation from Equation 16 to convert the tension inputs to stepper motor inputs.

$$\frac{2\pi}{360°} K_{dc}(k + k_c) = \frac{3}{2L}\frac{a}{b}\frac{T}{\theta} \quad (17)$$

Using nominal parameters in Equation 17 results in the prediction that K_{dc} = 0.012. From the step response data, it was found that K_{dc} is actually 0.015. This discrepancy is likely the result of the pipe's eccentricity, as well as nonlinearities in the system.

A state space model of the system was created using Equations 9 and 10 and the nominal system parameter values. The analytical state space equations and matrices are shown below.

$$\dot{\mathrm{x}} = A\mathrm{x} + Bu \tag{18}$$

$$y = C\mathrm{x} + Du \tag{19}$$

where $\mathrm{x} = \begin{bmatrix} \dot{\phi}_x \\ \dot{\phi}_y \\ \phi_x \\ \phi_y \end{bmatrix}$ $A = \begin{bmatrix} -\frac{B}{m_{eff}} & 0 & -\frac{(k+k_c)}{m_{eff}} & 0 \\ 0 & -\frac{B}{m_{eff}} & 0 & -\frac{(k+k_c)}{m_{eff}} \\ 1 & 0 & 0 & 0 \\ 0 & 1 & 0 & 0 \end{bmatrix}$

$B = -\frac{3}{2L} K_{dc}(k + k_c) \frac{a}{b} \frac{1}{m_{eff}} \begin{bmatrix} -1 & \frac{1}{2} & \frac{1}{2} \\ 0 & -\frac{\sqrt{3}}{2} & \frac{\sqrt{3}}{2} \\ 0 & 0 & 0 \\ 0 & 0 & 0 \end{bmatrix}$ $u = \begin{bmatrix} \theta_1 \\ \theta_2 \\ \theta_3 \end{bmatrix}$

$y = \begin{bmatrix} \phi_x \\ \phi_y \end{bmatrix}$ $C = \begin{bmatrix} 0 & 0 & 1 & 0 \\ 0 & 0 & 0 & 1 \end{bmatrix}$ $D = \begin{bmatrix} 0 & 0 & 0 \\ 0 & 0 & 0 \end{bmatrix}$

The state space model was used to simulate two step responses, one using the calculated gain value and the other using the experimentally derived gain value. The simulations were overlaid onto the high-pass-filtered step response data (Figure 2-3) for comparison between the model and reality.

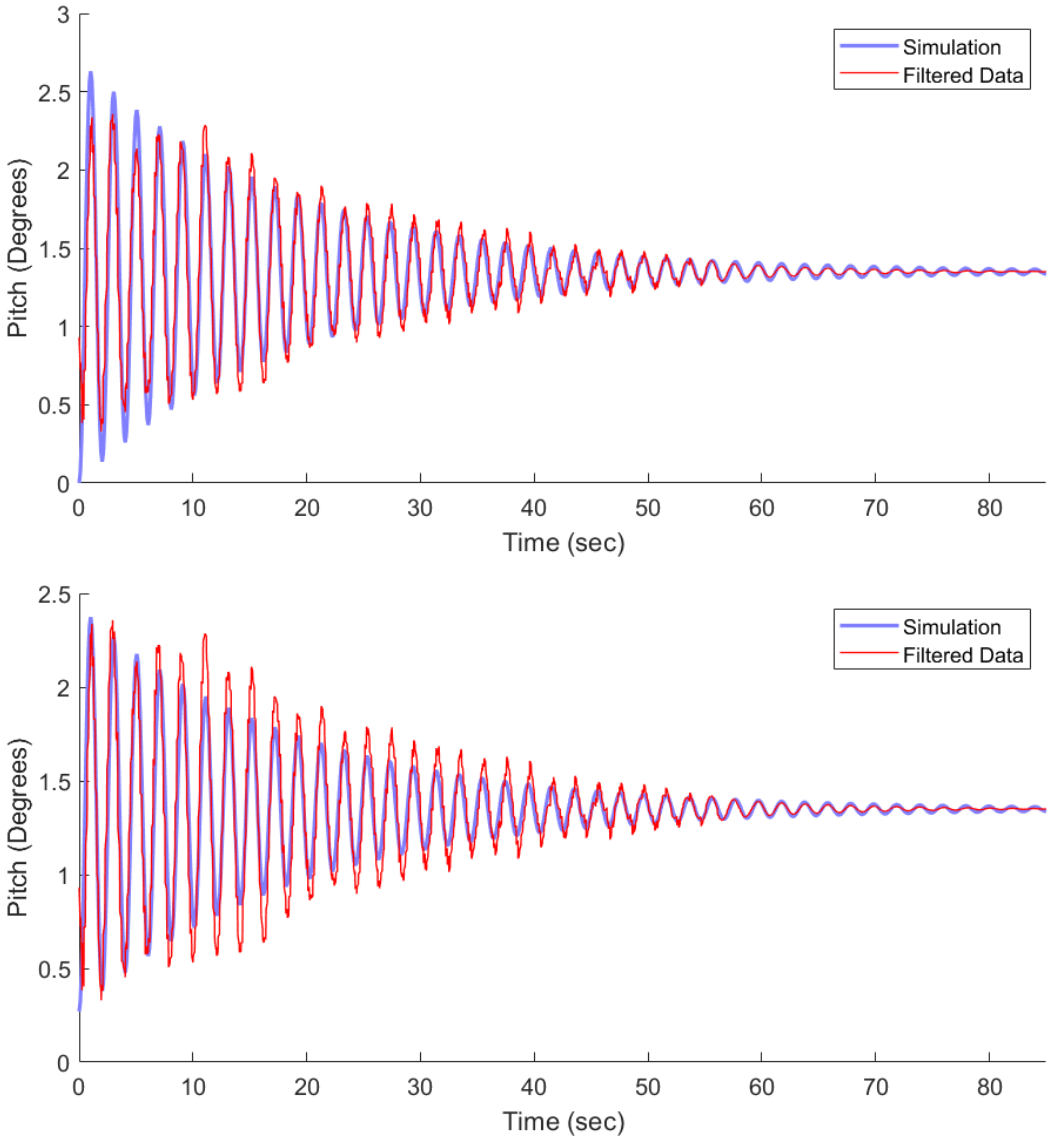

Figure 2-3. High-pass-filtered step response data overlaid onto the state space model simulations of the step response using nominal system parameters. The simulation represented in the upper plot uses the gain value obtained from the data, and the simulation in the lower plot uses the gain value calculated from nominal parameters.

2.4 Full-State Feedback

SELTI will only need to run the payload-positioning control system following the mast's deployment and whenever adjustment is required. When the control system achieves the targeted orientation, SELTI locks the winches to maintain the guyed system's state. There are few environmental disturbances on the lunar surface, so corrections should only be required occasionally. Therefore, the control system does not need to be quick.

On the contrary, a slow response with minimal overshoot is desired to prevent damage to hardware or tower collapse. With these considerations in mind, the chosen specifications for the physical model's control system were a settling time of 30 seconds and percent overshoot under 5%. To meet these specifications, second order time domain approximations (Equations 20 and 21) were used to find the desired closed loop poles.

$$T_s \approx \frac{4}{\zeta \omega_n} \tag{20}$$

$$OS \approx exp\left(-\frac{\pi \zeta}{\sqrt{1-\zeta^2}}\right) \tag{21}$$

where T_s is the settling time, and OS is the overshoot. The poles of a second order system are of the form $-\zeta\omega_n \pm \omega_n(1-\zeta^2)^{-2}\, i$. Using Equations 20 and 21, the desired closed loop poles of the system were found to be -0.14 ± 0.123. MATLAB was used to solve for the full state feedback gain matrix K_{fsf} that places the poles at these locations, with multiplicity 2.

Using the state space model with the gain matrix K_{fsf}, the closed loop responses to 90° winch rotation step inputs were simulated for each of the three guy wires. The simulations are shown in Figures 2-4 and 2-5.

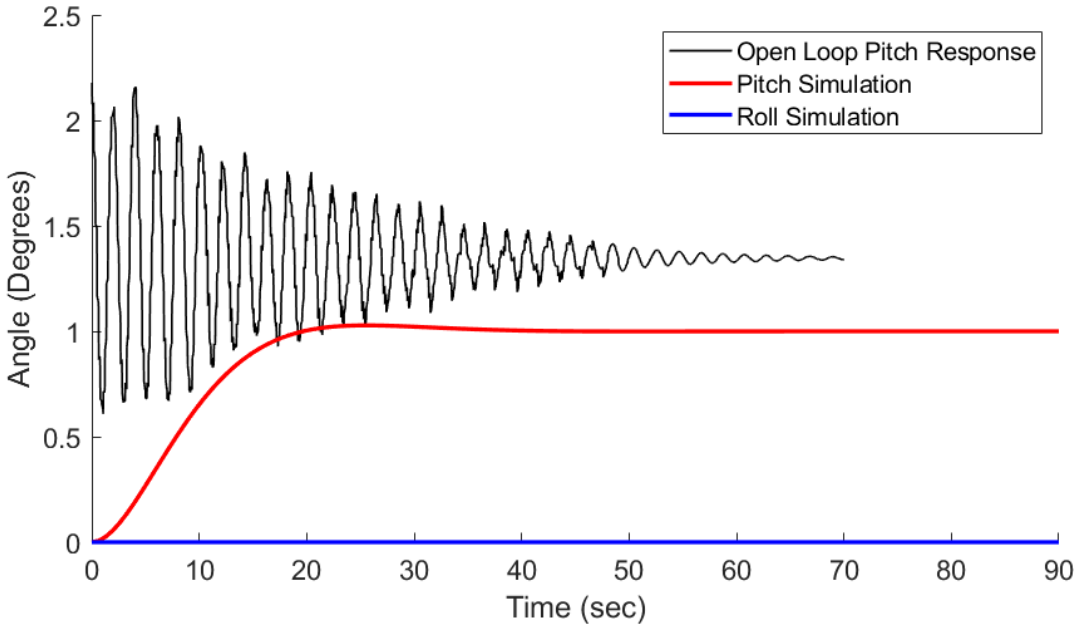

Figure 2-4. Open loop step response data and closed loop pitch and roll simulations for a 90° winch rotation step input in guy wire 1.

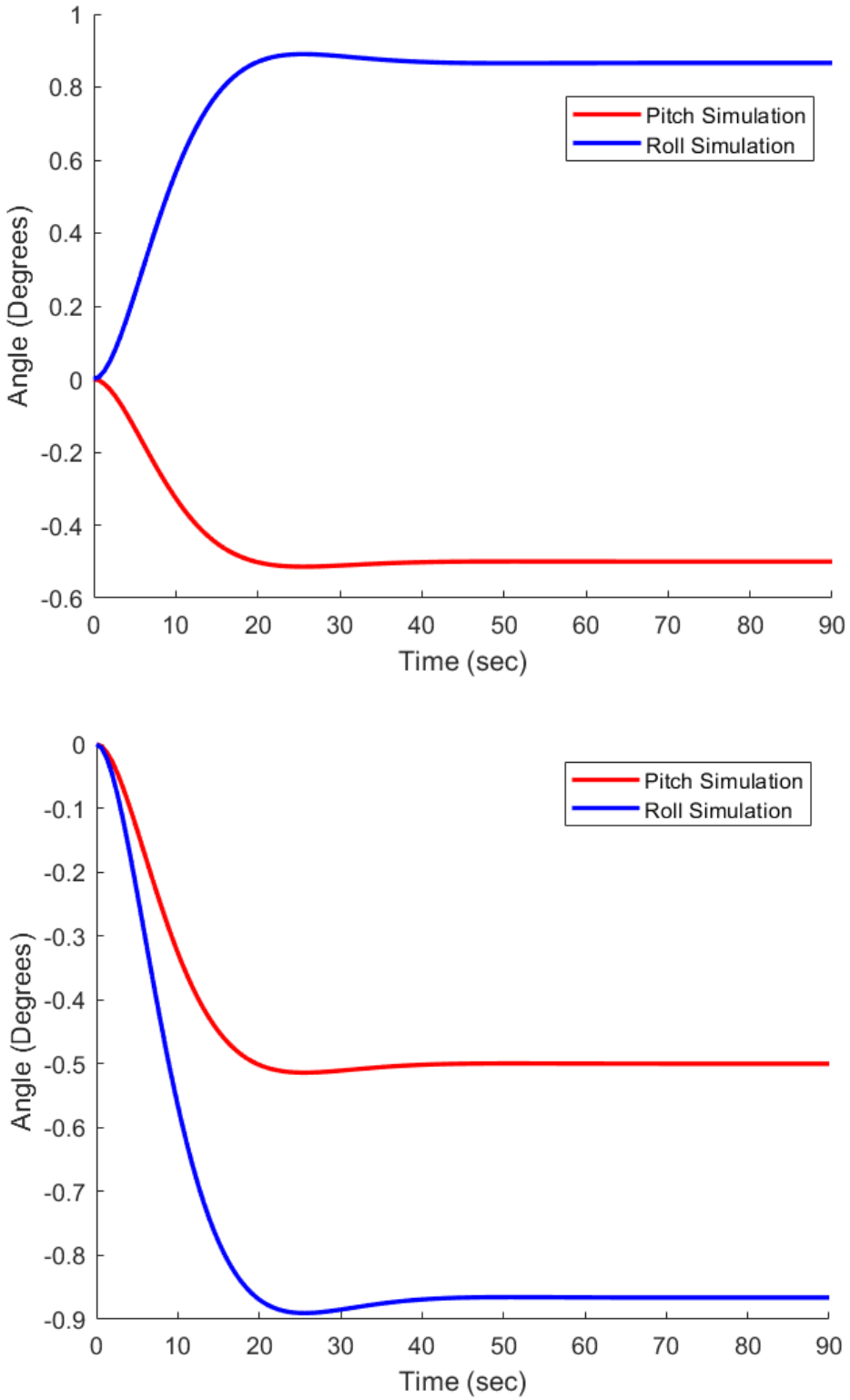

Figure 2-5. Closed loop pitch and roll simulations for 90° winch rotation step inputs in guy wire 2 (upper plot) and guy wire 3 (lower plot).

3. Discussion

3.1 Controller Performance

The closed loop state space simulations demonstrate that the controller meets the specifications, with settling times of about 31 seconds and percent overshoot under 3%. However, it is possible that the controller might not perform so well on the physical model. If the current controller gains result in actuator saturation, the system would behave nonlinearly, and the analytical model would fail. Nevertheless, the system's open loop and closed loop poles are stable, so the system will remain stable in the case of actuator saturation. Because SELTI deploys to such tall heights while having a narrow cross section, buckling and composite fracture are of great concern, so future control systems will need to implement tension limits for the guy wires, which will also introduce nonlinear effects that must be accounted for.

3.2 Analytical Model Limitations

Although the analytical model fits the step response data reasonably-well, it has several shortcomings due to its simplifying assumptions. The equations from Irvine [3] and the beam bending equations assume that the tower's tip displacements are small. However, SELTI and the model tower are known to experience deflections over 5% of their lengths, meaning that linear beam theory loses accuracy in this context. Furthermore, the guyed cable junction stiffness k_c from Huston et al. [4] is derived from equations that assume the cable ends are fixed to the ground rather than actuators. This can have a significant impact on the dynamics because k_c is not constant as the winches adjust tension. However, the resistance from opposing guy wires must be accounted for, and if the wire tensions remain close to the pretension value, it is a decent approximation of the guy wire dynamics.

3.3 Translation to SELTI

Using knowledge of the real tower and the scaling factors used for the physical model, the system identification experiments can be translated into an equivalent for SELTI. However, there are several inconsistencies between the physical model and the real tower that should be acknowledged. One significant difference is that SELTI's oscillations are greater in pitch than roll [1] due to the composite mast's different bending stiffnesses in the x- and y-directions. Due to the model tower pipe's radial symmetry, only the bending stiffness in one direction, the pitch, was scaled for the physical model. Nevertheless, the analytical model is able to account for the directional differences in stiffness, as the dynamics for each direction are handled separately.

Another discrepancy between the model and real tower are their eccentricities. The contour of the unloaded composite mast is not known and is caused by a variety of factors, including variations in the manufacturing process and the stowage method of wrapping it into a roll. The physical model is also eccentric, but in this case it is likely due to viscoelastic creep because the PVC pipe is constantly under the load of the mock payload. The physical model's eccentricity is in an arbitrary direction, whereas SELTI's eccentricity is heavily biased in the positive y-direction due to the lower bending stiffness and rolling direction during stowage.

4. Conclusions and Future Work

The system identification experiment data is consistent with the analytical model, suggesting that it is a valid approximation of the physical system. This validation will be useful for furthering the development of SELTI's payload position control.

The next step for this project is to continue controller design and simulation, checking for potential actuator saturation and assessing performance for various initial conditions and setpoints. After gaining confidence in the controller, it should be tested on the physical model to check for robustness. The effect of tension limits on controller performance should also be tested.

Once the controller performs well on the physical model, it can be adjusted for use on the real tower. The primary challenge in accomplishing this may be tuning the controller for the stiffer bending direction of the composite mast. The control system will also need to be adapted to accommodate various payload masses and tower deployment heights, as SELTI's dynamics will vary drastically as these variables change.

Other guy wire control systems should also be considered in the future. For example, SELTI's cable system can be used to keep the composite tower's center of mass centered during deployment to avoid tipping. Accomplishing this will be particularly challenging due the tower's changing height, which continuously alters system dynamics and wire tensions. Guy wire system controls could also be coordinated with the leveling system controls to optimize both payload position and center of mass.

References

[1] Miller, A. S., Lordos, G., Portmann, P., Studstill, A., Schoeman, W., Rorhbaugh, J., Williams, C., Rutherford, E., Zhang, J. Z., Patel, P. B., Weck, O. de, Hoffman, J., Martell, B. C., Stamler, N., and Fernandez, J. M., “Design Development of a Stable, Lightweight, Tall and Self-Deploying Lunar Tower,” Big Sky, MT.

[2] Irvine, H. M., 1992, *Cable Structures*, Dover Publications.

[3] “NASA: Artemis,” NASA [Online]. Available: https://www.nasa.gov/specials/artemis/index.html. [Accessed: 06-Apr-2023].

[4] Huston, D. R., Jr, W. B. S., Drzewiczewski, S., and Eid, B. F., 1998, “Position Stabilization of a Guyed Antenna Tower,” *Smart Structures and Materials 1998: Smart Structures and Integrated Systems*, SPIE, pp. 70–79.

[5] “Honeywell Spectra® 900 Fiber” [Online]. Available: https://www.matweb.com/search/datasheet.aspx?matguid=a01f54fb849147faa4da5dd8a635480b&ckck=1. [Accessed: 11-May-2023].

[6] Gurgoze, M., 2005, “On the Representation of a Cantilevered Beam Carrying a Tip Mass by an Equivalent Spring–Mass System,” Journal of Sound and Vibration - J SOUND VIB, **282**, pp. 538–542.